
PHYSICAL AND ENGINEERING FUNDAMENTALS
OF MICROELECTRONICS AND OPTOELECTRONICS

Molecular Beam Epitaxy of Strained Nanoheterostructures Based on Si, Ge, and Sn

A. S. Deryabin¹, A. E. Dolbak¹, M. Yu. Esin¹, V. I. Mashanov¹,
A. I. Nikiforov^{1*}, O. P. Pchelyakov¹, L. V. Sokolov¹, and V. A. Timofeev¹

¹*Rzhanov Institute of Semiconductor Physics, Siberian Branch, Russian Academy of Sciences,
Novosibirsk, 630090 Russia*

Received June 29, 2020; revised July 27, 2020; accepted July 31, 2020

Abstract—The results of investigating the generation of strained nanoheterostructures based on compounds with materials of group IV (Ge, Si, Sn) are presented. It is established how silver, tin, and lead atoms diffuse over the surface and what temperature dependences of diffusion coefficients are specific to atoms of these elements. It is shown that the diffusion of silver, tin, and lead atoms follows the mechanism of solid-phase wetting with generation of surface phases. The experimental data are provided that indicate the dominating role of edge dislocations and dislocation complexes of edge type in relaxation of Ge/Ge_{0.5}Si_{0.5}/Si(001) heterostructure. Tin-rich islands with Si pedestal on Si(001) substrate were obtained by the molecular beam epitaxy method. Firstly, the Sn film was applied on the Si surface. During the subsequent annealing an array of Sn islands, which were further used as catalysts for growing nanoobjects, was formed. Tin-rich islands with Si pedestal are formed after deposition of silicon at temperatures of 300–450°C on the surface with Sn islands. The growth of islands with pedestal occurred by the vapor–liquid–crystal mechanism. Intense photoluminescence was revealed from the tin-rich islands with Si pedestals in the wavelength range 1.3–1.7 μm.

DOI: 10.3103/S8756699020050039

Keywords: *heterostructures, Si, Ge, Sn, molecular beam epitaxy, diffusion, dislocations*

1. INTRODUCTION

The interest to the class of SiGeSn-based materials has significantly increased in recent years due to the possibility of fabrication of direct band-gap material and due to monolithic integration of electronic and photonic devices on a single silicon crystal [1–5]. Transition of the direct band-gap material occurs at a content of Sn from 6.5 to 11% for strain-relaxed GeSn films [6] and to 14.5% for GeSiSn films. Such contents considerably exceed the threshold of equilibrium solubility of Sn in Si and Ge. Creation of filamentary nanocrystals based on elements Ge, Si, and Sn of group IV allows overcoming the constraints related with Sn segregation, presence of defects, and mismatch of lattice parameters. To change the zone structure of filamentary nanocrystals, we may realize both radial and axial geometry of growth direction. The similar approaches were also used in forming filamentary nanocrystals in [6, 7]. Au is mostly used as a growth catalyst of filamentary nanocrystals of Si, Ge, or GeSi. Gold may serve as a trap for charge carriers; therefore, this mixture is disadvantageous for using in devices. Among others, Sn is proposed as an alternative variant of catalyst for growing filamentary Si and Ge nanocrystals [8]. Tin is more advantageous due to the low eutectic point (232°C), which is identified by the phase diagrams Si–Sn and Ge–Sn. Since Sn is a material of group IV, it can be embedded into the crystal lattice by replacing Si or Ge atoms. The main growth mechanism of filamentary nanocrystals based on Si and Ge is the vapor–liquid–crystal mechanism [9, 10].

For successful growth of filamentary nanocrystals we must take into account diffusion of atoms over the surface of semiconductors. There are several transfer mechanisms of atoms over the surface. If the

*E-mail: nikif@isp.nsc.ru

diffusion coefficients of atoms of substance over the clean surface are far less than that over the surface phase generated by these atoms, then the substance transfer is performed via the solid-phase wetting. In this case the atoms composing the surface phase are motionless. At achieving the front of distribution, the atoms diffusing over the surface phase come to the clean surface and form the surface phase, thus promoting the motion of the distribution front. The diffusion of Ag, Sn, and Pb over the Si(111) surface proceeds by this mechanism [11]. In contrast to the diffusion over the Si(111) surface, diffusion over the Ge(111) surface is investigated significantly worse.

Heterostructures (HS) with a large mismatch in lattice parameters, including the systems based on Ge, Si, and Sn, are characterized by a high density of defects of crystal lattice. This is caused by different mechanisms of stress relaxation influenced by lattice mismatch. One of ways for reducing the density of dislocations is the use of low-temperature buffer layers. The mechanisms of their generation and relaxation allow predicting the HS imperfection. Another way for improving crystalline perfection in heterostructures is the use of thin elastically strained layers in the pseudomorphic state. However, the thicknesses of these layers are limited by several nanometers. A dramatic reduction in density of defects may be obtained in filamentary nanocrystals of various geometry. Their dimensions reach hundreds of nanometers in diameter, and the crystalline imperfection is close to the parameters typical for the bulk material.

The stress field of an epitaxy film is usually relaxed by the mismatch dislocations (MDs), which are situated in the interface. They partially hold after the complete end of the relaxation process, which worsens the electronic properties of semiconductors. An important problem of epitaxy materials research is in reduced number of growing dislocations in the grown film. Its resolution requires a comprehensive study of the nature of penetrating dislocations and peculiarities of their relaxation. Lomer-type edge dislocations (L dislocations) are one of the main structural defects in crystals and films of Ge, Si, and A_3B_5 [12, 13]. In Ge/Si(001) heterostructures they are the dominating type of mismatch dislocations compensating the difference between the parameters of crystal lattice and substrate. L dislocations are formed as a result of joining of two complementary 60-deg MDs either at their accidental meeting or at the process of their induced generation [14]. Joining of two complementary 60-deg MDs in a single edge dislocation is an energetically favorable process, because the oppositely directed helical components of the Burgers vector of 60-deg MDs not participating in the process of plastic relaxation of the stressed film are counterbalanced. Computations of the specific energy of dislocation at atomic level show a significant energy gain at generation of an edge dislocation.

This work is aimed at analyzing the diffusion mechanism, the role of dislocations in stress relaxation and generation of strained nanoheterostructures based on compounds of materials of group IV by the MBE method.

2. DIFFUSION OF Ag, Sn, AND Pb OVER ATOMICALLY CLEAN SURFACES OF MOLECULAR BEAM EPITAXY OF Ge(111) AND Si(111)

Studying the diffusion of Ag, Sn, and Pb over atomically clean Ge(111) and Si(111) surfaces of molecular beam epitaxy was performed in the LAS-2000 setup (Riber, France). The surface structure was inspected by the low-energy electron diffraction method and the surface composition was inspected by the Auger electron spectroscopy. The concentration was computed following the model of uniform distribution of elements with the use of reference coefficients of elemental sensitivity. A strip with a thickness of ≈ 10 monolayers with a sharp boundary deposited on a clean surface of the sample was a source of metal atoms in studying the diffusion over the Ge surface. The measurement technique was presented in detail in [15]. At the Ge(111) surface we observed the concentration distributions after annealings.

The temperature dependence of the diffusion coefficients of silver atoms over Ge(111) and Si(111) surfaces is shown in Fig. 1 and described by

$$D_{\text{Ag/Ge(111)}} = 2.2e^{-0.9 \text{ eV}/kT} \text{ cm}^2/\text{s}, \quad D_{\text{Ag/Si(111)}} = 2.8 \times 10^2 e^{-1.2 \text{ eV}/kT} \text{ cm}^2/\text{s}.$$

The outflow of silver atoms from the surface to the bulk of germanium during annealing has no considerable effect on the form of concentration distributions, because its solubility in germanium is small in the studied temperature range. Diffusion of silver over the Si(111) and Ge(111) surfaces occurs

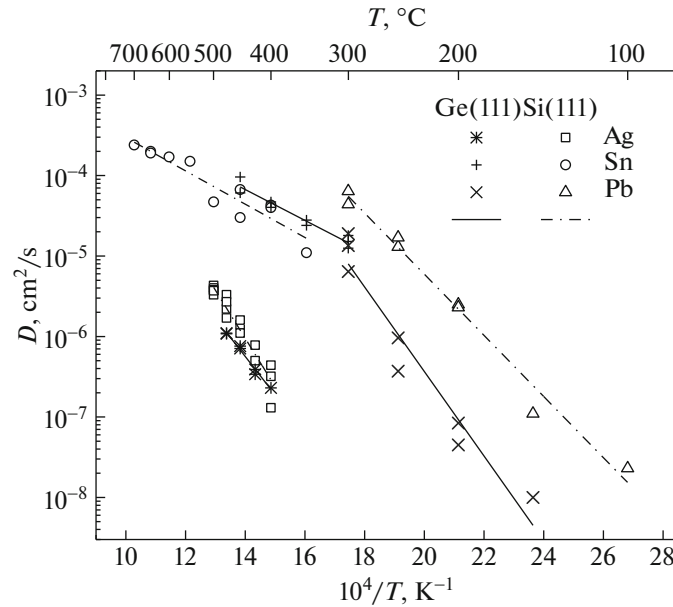


Fig. 1. Diffusion coefficients of Ag, Sn, and Pb over Ge(111) and Si(111) surfaces vs temperature.

by the mechanism of solid-phase wetting. The surface phases for Si(111) and Ge(111), over which silver atoms diffuse, are the same: $\sqrt{3} \times \sqrt{3}$ -Ag.

The concentration distributions of tin $C_{\text{Sn}}(x, t)$ over the Ge(111) surface were obtained in the temperature range 300–450°C. The shape of distributions corresponds to the diffusion by the mechanism of solid-phase wetting. On the surface occupied by the distribution, we observed the $3\sqrt{2}\sqrt{3}$ -Sn structure. The obtained diffusion coefficients were independent of annealing time at the same temperature. This indicates the fact that the source of tin atoms is a source of constant power and the diffusion in the bulk of germanium and the desorption of tin atoms from the surface have no substantial effect on the concentration distributions in the considered temperature range. The temperature dependence of the tin diffusion coefficients over the Ge(111) and Si(111) surfaces is presented in Fig. 1 and described by

$$D_{\text{Sn}/\text{Ge}(111)} = 5 \times 10^{-2} e^{-0.4 \text{ eV}/kT} \text{ cm}^2/\text{s}, \quad D_{\text{Sn}/\text{Si}(111)} = 3 \times 10^{-2} e^{-0.4 \text{ eV}/kT} \text{ cm}^2/\text{s}.$$

Thus, tin diffusion over the Si(111) and Ge(111) surfaces follows the mechanism of solid-phase wetting. Here, the structures formed on the silicon and germanium surfaces are different: Si(111)- $2\sqrt{3} \times 2\sqrt{3}$ -Sn and Ge(111)- $3 \times 2\sqrt{3}$ -Sn. The temperature dependences of the tin diffusion over the Si(111) and Ge(111) surfaces are practically identical. The surface phases Si(111)- $2\sqrt{3} \times 2\sqrt{3}$ -Sn and Ge(111)- $3 \times 2\sqrt{3}$ -Sn at a temperature of $\sim 200^\circ\text{C}$ are reversibly restructured with generation of the surface phases 1×1 -Sn [16]. Thus, diffusion of tin atoms over the silicon and germanium surfaces at temperatures higher than 200°C occurs not by the surface phases Si(111)- $2\sqrt{3} \times 2\sqrt{3}$ -Sn and Ge(111)- $3 \times 2\sqrt{3}$ -Sn, but by the phases 1×1 -Sn. We can suppose that the properties of the surface phases Si(111)- 1×1 -Sn and Ge(111)- 1×1 -Sn are close, which leads to practically identical coefficients and activation energies of diffusion.

Lead diffusion also follows the mechanism of solid-phase wetting. At the room temperature we observe the $\sqrt{3} \times \sqrt{3}$ -Pb structure on the surface occupied by the distribution. Heating to a temperature of approximately 300°C leads to reversible phase transition to the 1×1 -Pb structure.

The temperature dependence of the diffusion coefficients of lead is given in Fig. 1 and described by

$$D_{\text{Pb}/\text{Ge}(111)} = 5.3 \times 10^3 e^{-1.0 \text{ eV}/kT} \text{ cm}^2/\text{s}, \quad D_{\text{Pb}/\text{Si}(111)} = 800 e^{-0.8 \text{ eV}/kT} \text{ cm}^2/\text{s}.$$

The diffusion coefficients of lead over the Si(111) surface are by 1–2 orders of magnitude higher than that over Ge(111) in the temperature range 150– 300°C . The activation energies differ as well. This may be associated with peculiarities of the structure of surface superlattices $\sqrt{3} \times \sqrt{3}$ -Pb for silicon and germanium with the influence of low temperatures at which these peculiarities are significant.

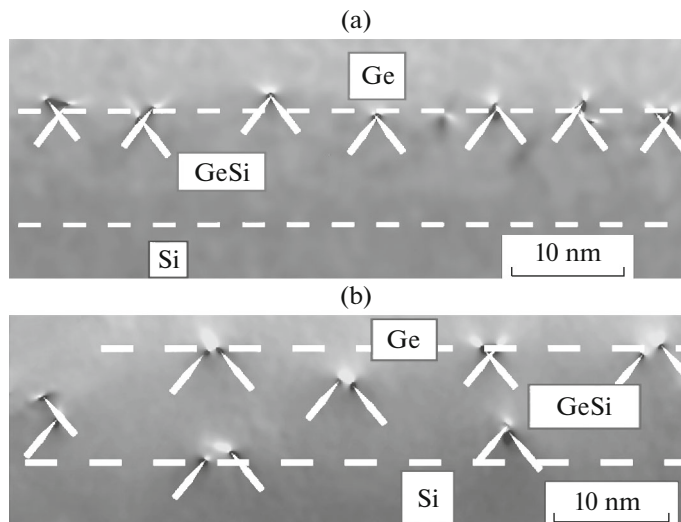


Fig. 2. Results of software processing of HREM images of Ge/Ge_{0.5}Si_{0.5} (10 nm)/Si(001) samples: (a) fresh grown sample (500°C) and (b) sample annealed at 600°C. The white arrows denote the ends of extraplanes {111} and the dashed lines denote the interfaces.

3. GENERATION OF DISLOCATION PAIRS IN Ge/GeSi/Si(001) HETEROSTRUCTURE

The Ge/LTGe/GeSi/Si(001) structures were grown by the molecular beam epitaxy method. At the surface of the Si substrate, we first grew a 10-nm GeSi buffer layer with a content of Ge equal to 0.5 at $T = 450^\circ\text{C}$ after that, we deposited a low-temperature Ge layer with a thickness of 7 nm at a low temperature ($T = 200^\circ\text{C}$). Then, simultaneously with the increase of temperature to $T = 500^\circ\text{C}$, we grew the main layer of Ge with a thickness of $0.5\ \mu\text{m}$. After the end of growth, the samples were annealed in hydrogen atmosphere at a temperature of 600 or 700°C during 10 min.

The dislocation structure of the grown samples was studied on transverse sections with a JEOL-4000EX electron microscope with an accelerating voltage of 400 kV. We used the high-resolution electron microscopy (HREM), the scanning transmission electron microscopy (STEM), and the software processing of HREM and STEM images.

As shown in [17], the parameters of the Ge/LTGe/GeSi/Si(001) heterostructures and the regimes of their growth may be selected so that the GeSi buffer layer remains pseudomorphic, the Ge film is generated on the artificial GeSi/Si(001) substrate, and the lateral parameter of its lattice repeats the lateral parameter of Si. In HSs of such type, after plastic relaxation of the Ge layer grown at 500° , almost all mismatch dislocations are of edge type and situated in the Ge/GeSi interface and the GeSi buffer layer remains pseudomorphic (Fig. 2a). At annealing of the HS a part of edge-type MDs, earlier considered motionless, migrate from the upper Ge/GeSi interface to the lower GeSi/Si interface (Fig. 2b). Such redistribution of edge dislocations between upper and lower interfaces is performed via motion of Lomer-type dislocation complexes [18].

At annealing, the Lomer-type dislocation defects are redistributed on two heterointerfaces so that the buffer layer mismatch is counterbalanced. Here, as a part of defects moves from the Ge/GeSi interface to the GeSi/Si interface, the fraction of dislocations with compact core is reduced in favor of loose dislocations with the core of 2–6 nm. Despite the increase in the distance between 60-deg dislocations generating an edge dislocation, in general, most 60-deg dislocations do not lose bounds, but generate a loose defect moving as a whole by the mechanism described in [19].

In the heterosystem of Ge on Si(001), the Lomer-type dislocations are formed from two 60-deg dislocations slipping along two glide planes {111} intersecting in the film/substrate interface. As a result of their interaction, an edge dislocation is generated. With regard to the GeSi/Si(001) system, four families of 60-deg dislocations propagate in each of two orthogonal directions $\langle 110 \rangle$: two families in each glide plane {111}. Antiparallel helical components of 60-deg dislocations are counterbalanced during interaction. Therefore, pairs of such dislocations, called complementary, are attracted to each

other and, when approaching is possible, are joined in compact Lomer-type edge dislocations. The interaction energy of complementary dislocations forming the Lomer-type one counts to ~ 27 eV/nm.

4. GENERATION OF FILAMENTARY NANOCRYSTALS BASED ON MATERIALS OF GROUP IV

All samples with elastically strained pseudomorphic GeSiSn layers and GeSiSn nanoislands were grown under conditions of ultrahigh vacuum 10^{-7} – 10^{-8} Pa on a Katun' S setup of molecular beam epitaxy. The MBE chamber was equipped with an electron beam evaporator for Si and Knudsen cell for Sn. The growth rates of Sn and Si layers were varied from 0.012 to 0.02 nm/s and from 0.53 to 1 nm/s, respectively. The growth and annealing temperatures were varied in the range 300–450°C. The Sn film on the Si surface was generated at the first stage and then annealed for creating arrays of Sn islands, which were used further as catalysts of growth of nanoobjects. The subsequent deposition of silicon on the surfaces with Sn islands led to appearance of Sn-rich islands with Si pedestals. The main method for inspecting morphology and structure of the surface was the high-energy electron diffraction (HEED). The transition from two-dimensional to three-dimensional film (2D–3D transition) at growth of Sn islands and appearance of Sn-rich islands with Si pedestals was controlled by variation in diffraction pattern. The film morphology was analyzed using the scanning electron microscope (SEM) (SU8220 by Hitachi, Japan). The SEM system allows performing elemental analysis of grown samples, because it additionally includes the EDX detectors (the energy-dispersive X-ray spectroscopy by Bruker, Germany). The optical properties of the sample were studied by the photoluminescence (PL) method. For PL excitation we used the YAG:Nd laser with a wavelength of 527 nm and a maximum power of 170 MW. We registered the photoluminescence by spectrometer based on double diffraction monochromator equipped with Ge detector. The PL measurements were carried out at liquid nitrogen temperature (77 K).

The technique for generating the HSs with strained GeSiSn layers was presented in detail in [20]. The epitaxy growth was performed on Si(100) substrates in the temperature range 150–450°C with the Sn content from 0 to 20%. Not only single GeSiSn layers, but also multilayer periodic structures containing GeSiSn/Si heterojunctions were obtained. Firstly, the GeSiSn layer was deposited and it was then covered by the Si layer with a thickness of 10 nm at a growth temperature of 400°C. Deposition of Sn layer on the Si(100) surface was carried out at a temperature of 100°C or at room temperature. The surface morphology was inspected by the HEED pattern. The polycrystal Sn film was generated, which corresponded to the HEED pattern with rings. The next stage of generation is annealing of Sn layer. During annealing we observed disappearance of rings corresponding to the polycrystal film and transition from the two-dimensional polycrystal film to the three-dimensional (2D–3D) one with Sn islands, which is accompanied by appearance of 3D reflexes on the HEED pattern. The maximum density of Sn islands achieved approximately 6×10^9 cm $^{-2}$. The obtained samples with Sn islands were used as a basis for Si deposition on them.

It is well-known that filamentary nanocrystals of Si are obtained mostly on Si(111) substrates; however, in works [21, 22] it was reported about growth of filamentary nanocrystals on Si(100). The surface tension of a catalyst drop increases in the direction from $\langle 100 \rangle$ to $\langle 111 \rangle$. Therefore, successful growth of filamentary nanocrystals is influenced by several factors such as growth parameters, orientation of substrate, and variation in eutectic point and compound of metal–Si catalyst drop. As a result of performed experiments, filamentary nanocrystals were not obtained in a pure form, as it is presented in the literature. It is related with peculiarities of growth on the (100) surface in the presence of tin as a catalyst. The growth of vertical filamentary nanocrystals on the (100) surface is realized with gold as a catalyst. However, it is anticipated that the use of (111) orientation as a substrate allows generating filamentary nanocrystals based on GeSiSn compounds in the presence of tin. We obtained tin-rich islands with pedestal with pyramidal lateral faces (Fig. 3). A part of islands disappears as a result of merging.

The elemental composition was studied by the energy-dispersive X-ray spectroscopy embedded in the SEM system. The pattern of the elemental composition obtained by this method is shown in Fig. 4. The Si and Sn elements correspond to blue and yellow colors, respectively. In addition, we may observe the traces of oxygen and carbon, which is associated with exposition of the sample in the atmosphere. We

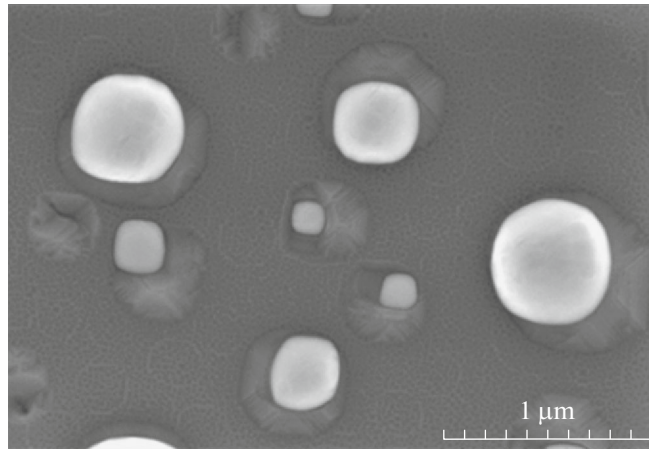


Fig. 3. SEM image of sample with tin-rich islands with pedestal.

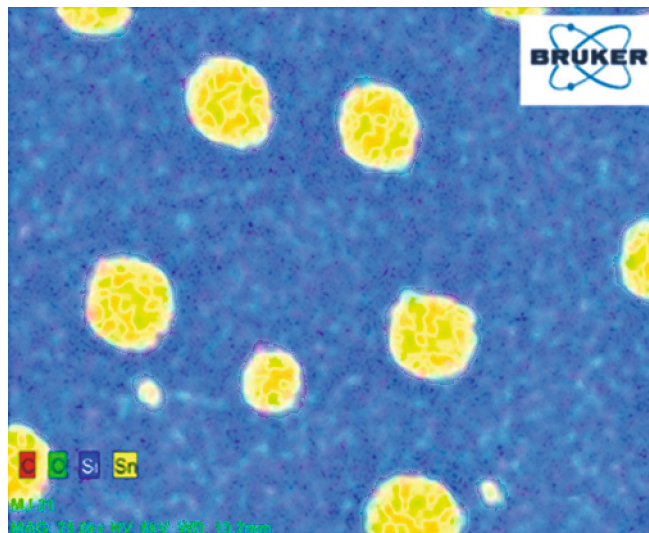


Fig. 4. Pattern of elemental composition obtained by the EDX method.

see in Fig. 4 that the pedestals are denoted by blue color; therefore, we may conclude that the pedestal contains Si.

The spectra of photoluminescence of the samples containing the Sn islands, the superlattice (SL) with the $\text{Si}/\text{Si}_{0.75}\text{Sn}_{0.25}$ heterojunction, and the tin-rich islands with pedestal are shown in Fig. 5. The sample including the superlattice and its spectrum obtained with X-ray diffractometry are provided in work [23]. The presence of satellites corresponding to the superlattice confirms the absence of dislocations. This sample was used for comparison with the samples containing Sn islands and tin-rich islands with Si pedestal. The photoluminescence spectrum of the samples with Sn islands does not show a significant signal in the range $1\text{--}1.7\ \mu\text{m}$. However, the sample with tin-rich islands with Si pedestal demonstrated an intense peak of PL in the range $1.3\text{--}1.7\ \mu\text{m}$. The PL signal of the sample containing the superlattice was observed also in the interval of wavelength from 1.3 to $1.7\ \mu\text{m}$, but it was weaker by 3 times. Since the sample with superlattice did not contain any dislocations and included pseudomorphic layers with $\text{Si}_{0.75}\text{Sn}_{0.25}$ compound, we may suppose that the solid solution SiSn is formed by solution of Si by tin.

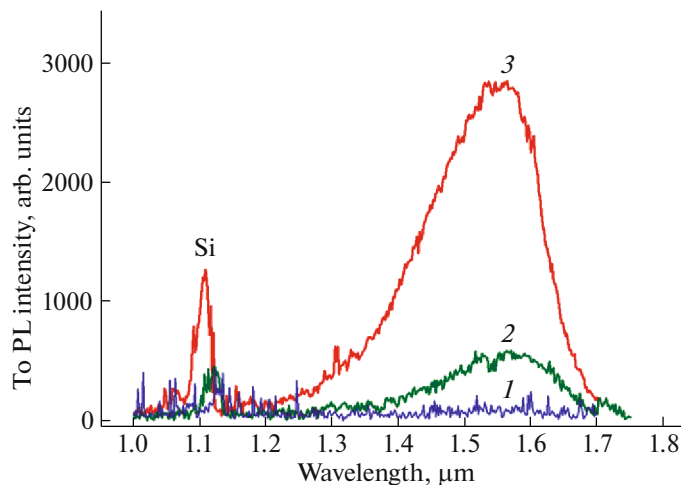


Fig. 5. Photoluminescence spectra of sample containing Sn islands (1), superlattice (SL) with Si/Si_{0.75}Sn_{0.25} heterojunction (2), and of sample with tin-rich islands with Si pedestal (3).

5. CONCLUSIONS

We established the diffusion mechanisms of silver, tin, and lead atoms over the Ge(111) surface and obtained the temperature dependences of the diffusion coefficients of atoms of these elements. It was shown that the diffusion of silver, tin, and lead atoms over the Ge(111) surface follows the mechanism of solid-phase wetting with formation of surface phases $\sqrt{3} \times \sqrt{3}$ -Ag, 1×1 -Sn, and $\sqrt{3} \times \sqrt{3}$ -Pb, respectively. Thus, the diffusion mechanisms of Ag, Sn, and Pb atoms and the surface phases generated by them in diffusion distributions coincide for the Ge(111) and Si(111) surfaces.

The provided experimental data demonstrate the dominating role of edge dislocations and edge-type dislocation complexes in the relaxation of the Ge/Ge_{0.5}Si_{0.5}/Si(001) heterostructure. Nevertheless, a small amount of dislocation configurations are met that consist of two non-complementary 60-degree dislocations with a uniaxial helical component. The total Burgers vector of such defect has the value of the type $a_0\langle 100 \rangle$.

The tin-rich islands with Si pedestal on the Si(100) substrate were obtained by the molecular beam epitaxy method. They are generated after deposition of silicon at the temperatures ranged from 300–450°C on the surface with Sn islands. The growth of islands with pedestal occurred by the vapor–liquid–crystal mechanism. The chemical analysis showed the presence of tin-rich region at the apex of nanoobjects. We observed an intense photoluminescence from tin-rich islands with Si pedestals in the range 1.3–1.7 μm.

REFERENCES

1. M. R. Bauer, J. Tolle, C. Bungay, A. V. G. Chizmeshya, D. J. Smith, J. Menéndez, and J. Kouvetakis, "Tunable band structure in diamond–cubic tin–germanium alloys grown on silicon substrates," *Solid State Commun.* **127**, 355–359 (2003). [https://doi.org/10.1016/S0038-1098\(03\)00446-0](https://doi.org/10.1016/S0038-1098(03)00446-0)
2. S. Wirths, R. Geiger, N. von den Driesch, G. Mussler, T. Stoica, S. Mantl, Z. Ikonik, M. Luysberg, S. Chiussi, J. M. Hartmann, H. Sigg, J. Faist, D. Buca, and D. Grutzmacher, "Lasing in direct-bandgap GeSn alloy grown on Si," *Nature Photon.* **9**, 88–92 (2015). <https://doi.org/10.1038/nphoton.2014.321>
3. A. Mosleh, M. A. Alher, L. C. Cousar, W. Du, S. A. Ghetmiri, Th. Pham, J. M. Grant, G. Sun, R. A. Soref, B. Li, H. A. Naseem, and Sh.-Q. Yu, "Direct growth of Ge_{1-x}Sn_x films on Si using a cold-wall ultra-high vacuum chemical-vapor-deposition system," *Front. Mater.* **2**, 30 (2015). <https://doi.org/10.3389/fmats.2015.00030>
4. R. Chen, S. Gupta, Y.-Ch. Huang, Y. Huo, Ch. W. Rudy, E. Sanchez, Y. Kim, Th. I. Kamins, K. C. Saraswat, and J. S. Harris, "Demonstration of a Ge/GeSn/Ge quantum-well microdisk resonator on silicon: enabling high-quality Ge (Sn) materials for micro-and nanophotonics," *Nano Lett.* **14**, 37–43 (2014). <https://doi.org/10.1021/nl402815v>
5. S. Gupta, B. Magyari-Köpe, Yo. Nishi, and K. C. Saraswat, "Achieving direct band gap in germanium through integration of Sn alloying and external strain," *J. Appl. Phys.* **113**, 073707 (2013). <https://doi.org/10.1063/1.4792649>

6. H. Y. Hui, M. de la Mata, J. Arbiol, and M. A. Filler, "Low-temperature growth of axial Si/Ge nanowire heterostructures enabled by trisilane," *Chem. Mater.* **29**, 3397–3402 (2017). <https://doi.org/10.1021/acs.chemmater.6b03952>
7. S. Assali, A. Dijkstra, A. Li, S. Koelling, M. A. Verheijen, L. Gagliano, N. von den Driesch, D. Buca, P. M. Koenraad, J. E. M. Haverkort, and E. P. A. M. Bakkers, "Growth and optical properties of direct band gap Ge/Ge_{0.87}Sn_{0.13} Core/Shell nanowire arrays," *Nano Lett.* **17**, 1538–1544 (2017). <https://doi.org/10.1021/acs.nanolett.6b04627>
8. M. Jeon, H. Uchiyama, and K. Kamisako, "Characterization of Tin-catalyzed silicon nanowires synthesized by the hydrogen radical-assisted deposition method," *Mater. Lett.* **63**, 246–248 (2009). <https://doi.org/10.1016/j.matlet.2008.10.005>
9. R. S. Wagner and W. C. Ellis, "Vapor-liquid-solid mechanism of single crystal growth," *Appl. Phys. Lett.* **4**, 89–90 (1964). <https://doi.org/10.1063/1.1753975>
10. E. I. Givargizov, "Fundamental aspects of VLS growth," *J. Crystal Growth.* **31**, 20–30 (1975). [https://doi.org/10.1016/0022-0248\(75\)90105-0](https://doi.org/10.1016/0022-0248(75)90105-0)
11. A. E. Dolbak and B. Z. Ol'shanetskii, "Diffusion of silver over atomically clean silicon surfaces," *J. Exp. Theor. Phys.* **143**, 952–956 (2013). <https://doi.org/10.1134/S1063776113060046>
12. W. M. Lomer, "A dislocation reaction in the face-centred cubic lattice," *Philos. Mag.* **42**, 1327–1331 (1951). <https://doi.org/10.1080/14786444108561389>
13. S. Mader, A. E. Blakeslee, and J. Angilello, "The interpretation of dislocation contrast in x-ray topographs of GaAs_{1-x}P_x," *J. Appl. Phys.* **45**, 4730–4734 (1974). <https://doi.org/10.1063/1.1663126>
14. E. P. Kvam, D. M. Maher, and C. J. Humphreys, "Variation of dislocation morphology with strain in Ge_xSi_{1-x} epilayers on (100) Si," *J. Mater. Res.* **5**, 1900–1907 (1990). <https://doi.org/10.1557/JMR.1990.1900>
15. A. E. Dolbak and R. A. Zhachuk, "Diffusion of Ag, Sn, and Pb over atomically clean Ge(111) surface," *J. Exp. Theor. Phys.* **129**, 391–396 (2019). <https://doi.org/10.1134/S1063776119080028>
16. T. Ichikawa, "Structural study of ultrathin Sn layers deposited onto Ge(111) and Si(111) surfaces by RHEED," *Surf. Sci.* **140**, 37–63 (1984). [https://doi.org/10.1016/0039-6028\(84\)90380-7](https://doi.org/10.1016/0039-6028(84)90380-7)
17. Yu. B. Bolkhovityanov, A. S. Deryabin, A. K. Gutakovskii, L. V. Sokolov, and A. P. Vasilenko, "Dislocation interaction of layers in the Ge/Ge-seed/Ge_xSi_{1-x}/Si(001) ($x = 0.3-0.5$) system: trapping of misfit dislocations on the Ge-seed/GeSi interface," *Acta Mater.* **61**, 617–621 (2013). <https://doi.org/10.1016/j.actamat.2013.05.028>
18. Yu. B. Bolkhovityanov, A. S. Deryabin, A. K. Gutakovskii, and L. V. Sokolov, "Unzipping and movement of Lomer-type edge dislocations in Ge/GeSi/Si(001) heterostructures," *J. Cryst. Growth* **483**, 265–268 (2018). <https://doi.org/>
19. Y. B. Bolkhovityanov, A. S. Deryabin, A. K. Gutakovskii, and L. V. Sokolov, "Unexpected travel of Lomer-type dislocations in Ge/Ge_xSi_{1-x}/Si(001) heterostructures," *Thin Solid Films* **616**, 348–350 (2016). <https://doi.org/10.1016/j.tsf.2016.08.058>
20. A. I. Nikiforov, V. A. Timofeev, V. I. Mashanov, T. A. Gavrilova, and D. V. Gulyaev, "Elastically stressed pseudomorphic SiSn island array formation with a pedestal on the Si(100) substrate using Sn as a growth catalyst," *J. Cryst. Growth* **518**, 103–107 (2019). <https://doi.org/10.1016/j.jcrysgro.2019.04.021>
21. R. R. Kumar, K. N. Rao, K. Rajanna, and A. R. Phani, "Growth of tin catalyzed silicon nanowires by electron beam evaporation," *Adv. Mat. Lett.* **4**, 836–840 (2013). <https://doi.org/10.5185/amlett.2013.3449>
22. V. Schmidt, S. Senz, and U. Gösele, "Diameter-dependent growth direction of epitaxial silicon nanowires," *Nano Lett.* **5**, 931–935 (2005). <https://doi.org/10.1021/nl050462g>
23. V. A. Timofeev, A. I. Nikiforov, A. R. Tuktamyshev, V. I. Mashanov, I. D. Loshkarev, A. A. Bloskin, and A. K. Gutakovskii, "Pseudomorphic GeSiSn, SiSn and Ge layers in strained heterostructures," *Nanotechnology* **29**, P. 154002 (2018). <https://doi.org/10.1088/1361-6528/aaac45>

Translated by E. Oborin